The American Journal of Pathology, Vol. 179, No. 3, September 2011

DOI: 10.1016/j.ajpath.2011.05.056

Tumorigenesis and Neoplastic Progression

Telomere Length Is Related to Alternative Splice Patterns of Telomerase in Thyroid Tumors

Yongchun Wang,* Alan K. Meeker,†‡ Jeanne Kowalski,§ Hua-Ling Tsai,§ Helina Somervell,* Christopher Heaphy,† Lauren E. Sangenario,* Nijaguna Prasad,* William H. Westra,† Martha A. Zeiger,*‡ and Christopher B. Umbricht*†‡

From the Departments of Surgery, Pathology,† and Oncology,‡ and the Division of Biostatistics,§ The Johns Hopkins Medical Institutions, Baltimore, Maryland*

Telomere dysfunction and aberrant telomerase expression play important roles in tumorigenesis. In thyroid tumors, three possibly inhibitory splice variants of the active full-length isoform of human telomerase reverse transcriptase (*hTERT*) may be expressed. These variants might regulate telomerase activity and telomere length because it is the fraction of the full-length isoform, rather than the total transcript level, that correlates with enzymatic activity. Telomerase reactivation may be critical in the early stages of tumorigenesis, when progressive telomere shortening may be limiting cell viability. The aim of this study was to investigate the relationship between telomere length and *hTERT* splice variant expression patterns in benign and well-differentiated malignant thyroid tumors. Telomere lengths of 61 thyroid tumors were examined by fluorescence *in situ* hybridization, comparing tumors with adjacent normal thyroid tissue on the same slide. Expression patterns of *hTERT* splice variants were evaluated by quantitative and nested RT-PCR. Telomere length was inversely correlated with percentage of full-length *hTERT* expression rather than with total *hTERT* expression levels. Short telomeres and high fractions of full-length *hTERT* transcripts were associated with follicular and papillary thyroid carcinomas, whereas long telomeres and low levels of full-length *hTERT* were associated with benign thyroid nodules. Intermediate levels of full-length *hTERT* and telomere length were found in follicular variant of papillary thyroid carcinomas and follicular adenomas. *(Am J Pathol 2011, 179: 1415–1424; DOI: 10.1016/j.ajpath.2011.05.056)*

Palpable thyroid nodules are present in almost 10% of the population, and the incidence of thyroid cancer has almost doubled in the United States in the past decade, increasing from 6.76 per 100,000 in 1997 to 11.99 per 100,000 in 2007.[1] A recent study on 30,766 differentiated thyroid cancer cases reported in the National Cancer Institute's Surveillance Epidemiology and End Results database between 1988 and 2005 found an increased incidence across all tumor sizes,[2] suggesting that the increasing incidence of thyroid cancer is not due to bias from an increased detection of smaller tumors. The study also shows that the survival rates of patients with thyroid cancer have not improved in the same period.

Fine-needle aspiration (FNA) cytology is currently the best diagnostic tool in the differential diagnosis of a thyroid tumor, but it often cannot differentiate a benign from a malignant lesion, resulting in up to 30% ambiguous and nondiagnostic FNA results.[3] Thyroidectomy is recommended for the treatment of most thyroid cancers.[4–6] However, thyroidectomy for all patients with suspicious FNA at the first operation is unacceptable because up to 50% of lesions suspicious for thyroid cancer and 80% of all follicular neoplasms are ultimately benign.[7–11] Conversely, performing unilateral lobectomy alone for all suspicious lesions may require a completion thyroidectomy days after an initial operation, a practice considerably riskier than a single operation. Patients with a suspicious FNA diagnosis, therefore, pose a serious clinical dilemma.[12]

Complicating this picture, there is considerable interobserver and intraobserver variability in the classification of follicular lesions.[13] Although significant efforts have been made to define the molecular features of the various thyroid tumor subtypes, which should allow improved classification based on the underlying molecular changes, we currently lack reliable tools to accomplish this. Therefore, further investigations are needed to identify the defining mechanisms responsible for the thyroid carcinogenesis and tumor progression of the different tumor subtypes.

Supported in part by grants from the National Institutes of Health (R21 CA137550) and the American Cancer Society (RSG-08-003-01-CCE).

Accepted for publication May 11, 2011.

Address reprint requests to Christopher B. Umbricht, M.D., Ph.D., Department of Surgery, The Johns Hopkins University School of Medicine, 720 Rutland Ave., Ross 743, Baltimore, MD 21205. E-mail: cumbrich@jhmi.edu.

Telomeres constitute the ends of eukaryotic chromosomes and are composed of 1000 to 2000 tandem repeats of the hexanucleotide sequence TTAGGG; they progressively shorten in somatic cells during each cell cycle until apoptosis or cell cycle arrest is triggered.[14] Possible functions of telomeres include prevention of chromosome degradation, end-to-end fusions, chromosomal rearrangements, and chromosome loss.[15] The stabilization of telomere length plays an important role in tumorigenesis,[16] and the maintenance of telomeres is a prerequisite for malignant tumors to preserve their ability to proliferate. Nevertheless, significant telomere shortening has been reported despite detectable telomerase activity in numerous cancer tissues, including lung, breast, colon, pancreas, and prostate,[17–21] indicating that even when malignant cells can reactivate telomerase and escape the constraints of critical telomere shortening, pre-immortalization telomere shortening may not be completely reversible.

Two mechanisms maintain telomere length. Cancer cells commonly maintain telomere length by strictly regulating telomerase expression and/or catalytic activity. An alternative mechanism consists of lengthening telomeres by recombination-mediated DNA replication, although the latter mechanism is more prevalent in tumors arising from mesenchymal tissues than in epithelial tumors, such as thyroid cancer.[22,23] Most human epithelial cancers, including thyroid cancers, have been shown to have short telomeres, despite the presence of detectable telomerase activity.[20,24]

Human telomerase consists of a ribonucleoprotein containing a protein catalytic subunit, the human telomerase reverse transcriptase (*hTERT*), and an RNA component, the human telomerase RNA, and it may require dimerization or multimerization for optimal activity.[25,26] The *hTERT* transcript is known to have seven alternative splice sites, which can theoretically produce multiple tissue- and disease-specific alternative transcripts,[27,28] only a few of which have been well documented to date, however. We recently identified four *hTERT* splice transcript variants in thyroid tumors: full-length, α-deletion, β-deletion, and α-β-deletion transcripts.[29] We also looked for the other possible *hTERT* splice variants in thyroid tumors but did not find any evidence of the other species, including the γ-deletion, which was identified in hepatocellular carcinoma cell lines. Telomerase enzyme activity was shown by several groups to depend on the presence of full-length *hTERT* gene expression.[30,31] The in-frame α-deletion (36 bp within the RT motif A)–derived protein is a dominant negative inhibitor of telomerase activity,[32–34] as would be expected if it forms heterodimers with the full-length transcript-derived protein. The reading-frameshifting β-deletion (182 bp) and α-β-deletion (218 bp) are believed to produce truncated proteins and may be subject to nonsense-mediated mRNA decay due to the premature stop codon.[33,35] A previous study on *hTERT* splice variants in thyroid tumors confirmed that it was the fraction or percentage of full-length transcript, rather than the overall level of *hTERT* expression, that correlated directly with enzymatic telomerase activity.[29] No study to date, however, has examined whether telomere length correlates with *hTERT* alternative splice variant patterns in thyroid tumors.

In this study, we used a fluorescence *in situ* hybridization (FISH)–based method to measure telomere length in 61 formalin-fixed, paraffin-embedded (FFPE) human thyroid tumors of 7 histologic subtypes, which are a subset of the series in which we previously reported the presence of *hTERT* splice variants.[29] This study included 34 malignant tumors: 15 papillary thyroid carcinomas (PTCs), 12 follicular variant of PTCs (FVPTCs), 4 follicular carcinomas (FCs), and 3 Hürthle cell carcinomas (HCs); and 27 benign lesions: 12 follicular adenomas (FAs), 6 Hürthle cell adenomas (HAs), and 9 adenomatoid nodules (ANs). Because FCs and HCs are relatively infrequent, resulting in limited sample numbers, we grouped follicular neoplasms with or without Hürthle cell morphologic features together for the statistical analyses.

We compared the relative telomere length in each thyroid tumor with *hTERT* splice variant patterns and found that, overall, telomere length correlated strongly with the percentage of full-length *hTERT* expressed rather than with its absolute expression level or the level of total *hTERT* transcription, including all splice variants. Furthermore, short or absent telomeres and high fractions of full-length *hTERT* were also associated with the FC and PTC tumor subtypes represented in the study cohort, which was limited to well-differentiated carcinomas and benign thyroid tumors.

Materials and Methods

Tissue Samples

Frozen tissues were used for RNA extraction, and the matched FFPE thyroid tissue sections were used for telomere FISH analysis. The frozen thyroid tumors were selected from an existing thyroid tissue bank, which has been approved by the Institutional Review Board at Johns Hopkins Medical Institutions. After obtaining informed consent, we collected thyroid tumor specimens for our tissue bank from patients undergoing thyroid surgery at Johns Hopkins Hospital. Samples were immediately placed on ice, prosected in the Department of Pathology from the centers of the lesions, snap frozen in liquid nitrogen, and stored at −80°C until use. The samples used in this study were collected between 1998 and 2005. H&E-stained cryosections were prepared from the frozen samples to ensure representative sampling from the tumors, defined as >75% tumor tissue. Unstained sections and a control H&E slide were obtained from the Department of Pathology FFPE tissue archive and were used for FISH analysis. The study pathologist confirmed all final surgical pathology diagnoses on cryosections and permanent sections.

Reverse Transcription and Nested PCR

Total RNA was isolated from each tumor using TRIzol (Invitrogen, Carlsbad, CA) and was purified using the RNeasy mini kit (Qiagen, Valencia, CA). Reverse transcription was performed with 1 μg of total RNA and 250 ng of random primers by SuperScript III reverse transcriptase (Invitrogen). The relative gene expression levels

of *hTERT* alternative splice variants were analyzed by nested PCR, as previously described.[29] The first round of PCR was maintained in the exponential phase. Amplified products were separated in 2% agarose gels with nucleic acid gel stain (Cambrex, Rockland, ME) and were visualized under UV light. The densitometric value of each *hTERT* transcript was quantified using Quantity One image analysis software (version 4.5.2; Bio-Rad, Hercules, CA). The relative gene expression level of each transcript was reported as a relative fraction of all the *hTERT* transcripts present in the same sample.[36] The nested PCR has been optimized using thyroid cell line RNAs to ensure no apparent distortion in the amplified products in each sample. *β-Actin* served as an internal control.

Real-Time PCR

Real-time PCR was performed in triplicate for each sample using iQ SYBR Green Supermix (Bio-Rad) and was analyzed on a Bio-Rad iQ5 thermal cycler. Total *hTERT* expression level was detected with primers 5′-GCTACGGCGACATGGAGA-3′ (forward) and 5′-GCGTGGGTGAGGTGAGGT-3′ (reverse), and the *hTERT* full-length transcript was detected with 5′-TACTTTGTCAAGGTGGATGTG-3′ (forward) and 5′-GCTGGAGGTCTGTCAAGGT-3′ (reverse). The expression level of *hTERT* was normalized to *β-Actin*.

Telomere FISH

To minimize the processing differences, every slide was recut from a paraffin-embedded tissue block containing thyroid neoplastic and adjacent normal thyroid tissue. Suitable areas were identified by light microscopy on H&E-stained slides before the FISH analysis, which was performed on a consecutive slide. The H&E-stained slide was used as a guide during evaluation of the adjacent telomere FISH slides. Hybridization to telomeric DNA using a directly labeled pan-telomeric peptide nucleic acid (PNA) FISH probe was performed without protease digestion, as previously described.[19,20] Briefly, 4-μm-thick sections from FFPE tissues were deparaffinized and hydrated through a graded ethanol series. Slides were then placed in citrate buffer (Vector Laboratories, Burlingame, CA), steamed for 14 minutes, and then dehydrated, followed by application of a Cy3-labeled telomere-specific PNA probe. This probe is complementary to the mammalian telomere repeat sequence and has the sequence (NH_2 terminus to COOH terminus) 5′-CCCTAACCCTAACCCTAA-3′ with an NH_2-terminal covalently linked Cy3 fluorescent dye. Samples were denatured for 4 minutes at 83°C, followed by a 2-hour room temperature hybridization step. As a control for hybridization efficiency, a fluorescein isothiocyanate–labeled PNA probe with the sequence 5′-ATTCGTTGGAAACGGGA-3′ and specificity for human centromeric DNA repeats (CENP-B binding sequence) was also included in the hybridization solution.[37] After hybridization, slides were washed to remove any unbound probe and were counterstained with the DNA binding dye DAPI (Sigma-Aldrich, St Louis, MO) at a concentration of 500 ng/mL in water. Slides were then rinsed well in deionized water, drained, mounted with ProLong antifade mounting medium (Molecular Probes Inc., Eugene, OR), and coverslipped. All the slides were imaged using a Nikon 50i epifluorescence microscope equipped with an X-Cite 120 series illuminator (EXFO Photonics Solutions Inc., Mississauga, ON, CA) and a 40× Neofluotar lens and appropriate fluorescence excitation/emission filter sets. Grayscale images were captured for presentation using NIS-Elements software (Nikon Instruments Inc., Melville, NY) and an attached CoolSNAP EZ digital camera (Photometrics, Tucson, AZ), pseudo-colored, and merged. All images were collected during a single imaging session, during which integration times were kept constant: 700 milliseconds for Cy3 (telomere) and fluorescein isothiocyanate (centromere) and 50 milliseconds for the DAPI counterstain. Telomere lengths were assessed by visually comparing telomere signals from tumor cells with telomere signals from adjacent normal thyroid tissue and were graded using the following 5-point scale: 0, very short; 1, notably shorter than normal; 2, similar to normal; 3, notably longer than normal; and 4, very long. Areas to be scored were selected by one investigator with the guidance of the consecutive deidentified H&E section, after which the scoring investigator examined the FISH slide in a blinded manner.

Reproducibility of Telomere FISH Scoring

Intraobserver and interobserver variability of the telomere length scoring method was assessed on a 55-sample breast cancer TMA, which was processed in an identical manner as the thyroid tumor series and was scored twice over 2 days by two observers using the same 5-point scale. As seen in Table 1, breast cancer telomeres show much higher levels of heterogeneity than is seen in well-differentiated thyroid carcinoma. Therefore, this represents a conservative assessment of the reproducibility in this study, where one observer performed the scoring.

Statistical Analysis

We examined the ability of the gene expression levels of *hTERT* and average telomere length, as assessed by FISH, separately and combined, to distinguish between benign (FAs, ANs, and HAs) and malignant (PTCs, FVPTCs, FCs, and HCs) thyroid tumor subtypes.

A logistic regression model was used to examine the statistical significance of *hTERT* splice variant expression and telomere length and the probability of the tumor being malignant or benign. Receiver operating characteristic (ROC) curves were constructed to examine the ability of the two best potential markers (percentage of

Table 1. Reproducibility of Telomere Length Scoring in Cancer TMAs

	Concordant scores	Discordant scores (±1)	Discordant scores (±1)
Intraobserver	50/55 (91%)	5/55 (9%)	0/55
Interobserver	46/55 (84%)	9/55 (16%)	0/55

full-length *hTERT* expression and telomere length), separately and combined, to distinguish between malignant and benign thyroid tumor subtypes. As an overall estimate of diagnostic performance, areas under the curve (AUCs) are reported and compared based on the method of DeLong et al.[38] In addition, sensitivity and specificity estimates, based on the value of each separate marker that maximizes specificity while retaining sensitivity >50%, are reported. Altogether, results from 61 tumors were examined: PTCs (n = 15), FVPTCs (n = 12), FCs (n = 4), HCs (n = 3), FAs (n = 12), HAs (n = 6), and ANs (n = 9). Undetectable *hTERT* expression was defined as no expression.

The JMP 7 statistical program (SAS Institute Inc., Cary, NC) was used for parametric and nonparametric tests comparing groups, including the Wilcoxon and Kruskal-Wallis rank sum tests, and for the bivariate linear fit and Spearman's rho tests for nonparametric correlations.

Results

Quantitation of Total hTERT Transcripts and Full-Length hTERT Transcripts in Thyroid Tumors

Expression levels of total *hTERT* and the full-length transcript were determined by quantitative RT-PCR. To measure total *hTERT*, gene-specific primers were designed to span a common sequence region shared by all four *hTERT* isoforms. To selectively measure the full-length isoform, primers were designed to encode sequences in the α- and β-deletion sites. As shown in Figure 1A, the expression level of total *hTERT* was higher in PTCs than in the other tumor types, although this did not reach statistical significance. When only full-length transcripts were considered, PTCs showed significantly higher levels than did FVPTCs and adenomas (Figure 1B). Except for one AN outlier case, ANs had significantly less full-length *hTERT* than did the other tumor subtypes.

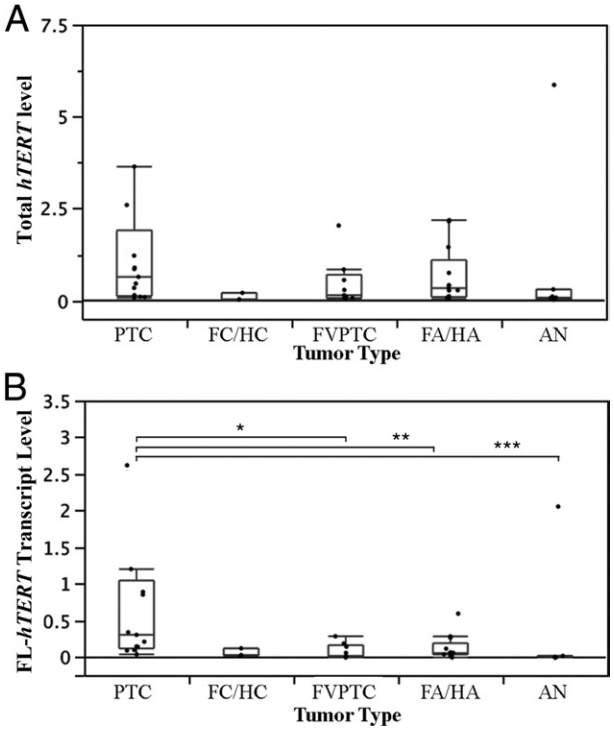

Figure 1. Box plots of *hTERT* expression levels as determined by quantitative RT-PCR in thyroid tumors. **A:** Total *hTERT* levels. One PTC outlier (*hTERT* = 17) is not shown. **B:** *hTERT* full-length transcript levels. One PTC outlier (FL-*hTERT* = 10) is not shown. Group comparisons using the Wilcoxon test showing a significant difference are indicated. $^{*}P < 0.04$, $^{**}P < 0.03$, and $^{***}P < 0.01$. **Box plot bars** indicate 25%, 50%, and 75% quartiles. **Whiskers** indicate 5th and 95th percentiles.

hTERT *Alternative Splice Variant Patterns in Thyroid Tumors*

We previously investigated the expression patterns of *hTERT* splice variants using nested primer sets designed to span a region that included the α- and β-deletion sites.[29] The splice variant assay was repeated for the subset of samples in this study to have a side-by-side comparison with the quantitative assessment of total *hTERT* transcript expression levels. Figure 2A is a representative agarose gel image showing the splice variant patterns of four of the most common thyroid tumor types. Using this highly sensitive nested RT-PCR assay, the total *hTERT*-positive rates were similar in the 34 malignant (82.35%) and 27 benign (85.19%) tumor samples. In contrast to overall *hTERT* expression, the full-length variant was expressed at significantly higher fraction levels in malignant tumors (mean ± SD: 50.26% ± 7.37% of total transcripts) than in benign tumors (mean ± SD: 18.47% ± 4.95% of total transcripts; $P < 0.002$). Furthermore, the full-length *hTERT* was expressed at high levels in PTCs and FCs/HCs and at considerably lower levels in FVPTCs and benign tumors (FAs/HAs and ANs). The decrease in full-length transcript expression was accompanied by a concomitant increase in the inhibitory α-deletion variant and the nonfunctional β-deletion variant in benign tumors (Figure 2B). The α-β-deletion variant was seen in only two HAs (2% and 15% of total transcripts, respectively). We grouped them with the β-deletion variant because both variants cause reading-frameshifts and would code for presumably inactive peptides.

Although neither total *hTERT* expression nor full-length isoform levels correlated with tumor subtypes, the relative fraction of full-length transcript, as expressed in percentage of total *hTERT* (%FL-*hTERT*; Figure 2C), seemed to classify the thyroid tumors into three distinct categories. The full-length transcript percentage was high in PTCs, HCs, and FCs; intermediate levels were found in FVPTCs, HAs, and FAs; and ANs had only a small fraction of full-length transcript.

Telomere Length in Thyroid Tumors

To investigate the relationship between telomere length and *hTERT* transcript levels and splice variant patterns detected by nested RT-PCR, we performed a FISH-based semiquantitative analysis of telomere ends on FFPE sections of the same thyroid tumor samples used to

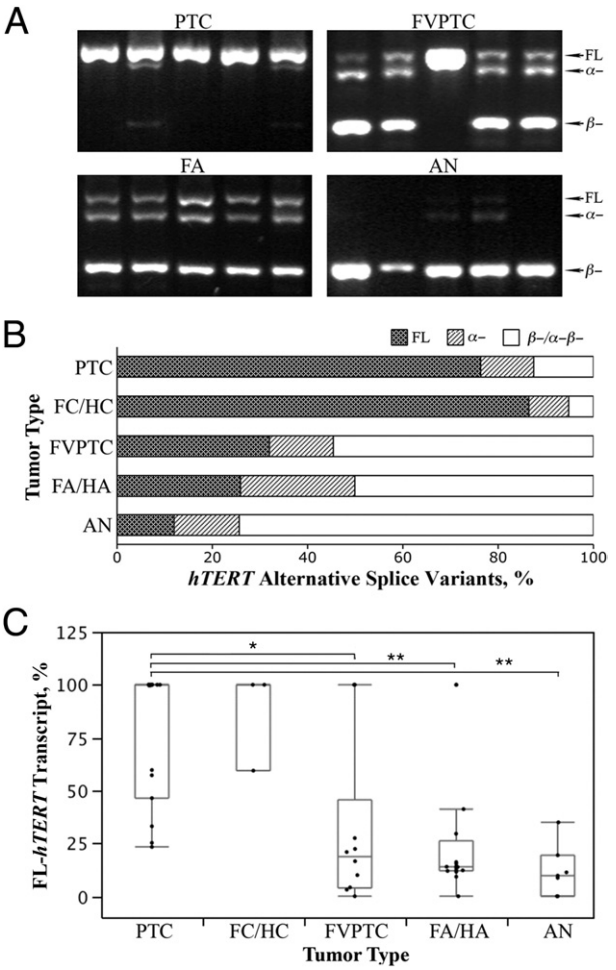

Figure 2. *hTERT* alternative splice variant patterns in thyroid tumors. **A:** Representative electrophoretic patterns of nested RT-PCR of *hTERT* alternative splice variant patterns present in PTC, FVPTC, FA, and AN. **B:** *hTERT* splice variant patterns in the seven most common thyroid tumor types. The α-β-deletion variant was seen in only two HAs (2% and 15% of total transcripts, respectively) and was grouped in the β-deletion. **C:** %FL-*hTERT* in thyroid tumors. Group comparisons using the Wilcoxon test showing a significant difference are indicated except for the FC/HC group because of its low case count. $^{*}P < 0.03$, $^{**}P < 0.01$. **Box plot bars** indicate 25%, 50%, and 75% quartiles. **Whiskers** indicate 5th and 95th percentiles.

determine *hTERT* expression levels. To ensure an unbiased assessment and direct comparison of tumor and matching normal thyroid epithelium, slides were prepared from tissue blocks containing thyroid neoplastic and adjacent normal tissue, as identified on a consecutive H&E-stained slide. Telomere FISH analysis was performed in a blinded manner. Figure 3, A and B show telomeres (stained red) in a case of PTC and a case of FA with their adjacent normal thyroid tissues. The blue-colored centromeric DNA served as internal reference. The samples were processed in batches containing all the tumor subtypes to limit potential processing differences.

Of the malignant subgroups, 12 of 15 PTCs (80%), 1 of 4 FCs (25%), all 3 HCs (100%), and 4 of 12 FVPTCs (33%) had very short telomeres compared with the adjacent normal thyroid tissue. The remainder of the carcinomas had telomere lengths similar to those of normal thyroid tissue (Table 2). Of the benign follicular neoplastic subgroups, 6 of 12 FAs (50%) and 1 of 6 HAs (17%) had shorter telomeres. In hyperplastic (AN) tumors, 2 of 9 (22%) had short telomeres. All other benign tumors had lengths similar to (score = 2) or longer than (score = 3) adjacent normal thyroid tissue (Table 2).

As summarized in Figure 3C, PTCs had the shortest telomeres of all subgroups, whereas ANs had the longest telomeres. The various follicular neoplastic subtypes (FVPTC, FA, and HA) fell into an intermediate range of telomere lengths.

The relationship between telomere length and expression of the *hTERT* splice variants was analyzed further by quantitative RT-PCR. The fraction of full-length *hTERT*, expressed as percentage of total *hTERT*, was determined using nested PCR as discussed previously. No correlation was found between total *hTERT* expression levels and telomere length, and the correlation between telomere length and full-length *hTERT* expression levels did not reach statistical significance (Figure 4, A and B). A significant correlation was found, however, between the

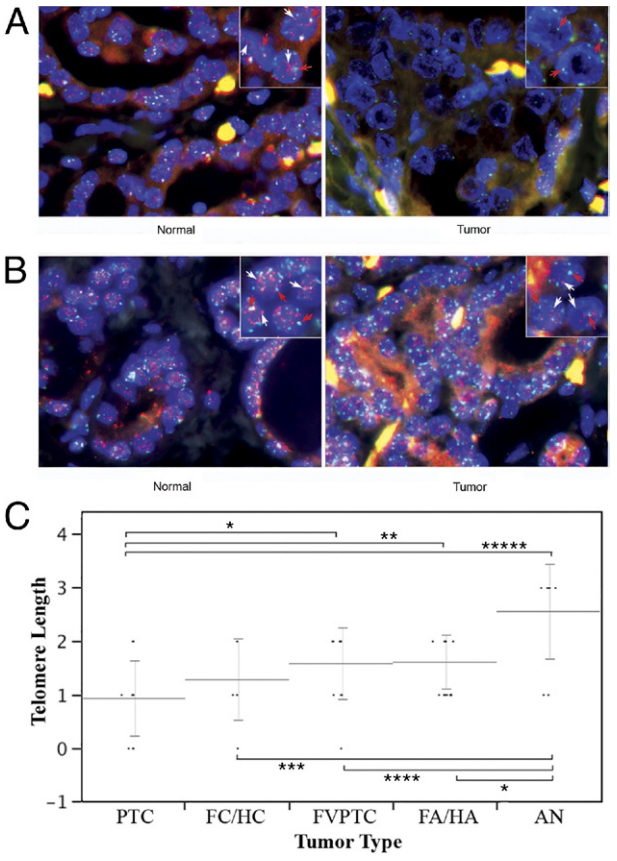

Figure 3. Telomere length in thyroid tumors and adjacent normal thyroid tissue. **Insets: White arrows** indicate red-colored telomeric DNA; **red arrows**, blue-colored centromeric DNA. **A:** PTC and adjacent normal thyroid. Original magnification, ×40. The case had 100% FL-*hTERT* transcript. The telomere length was 0, very short compared with the adjacent normal thyroid tissue. **B:** FA and adjacent normal thyroid. Original magnification, ×40. The case had 14% full-length, 18% α-deletion, and 68% β-deletion *hTERT* transcripts. The telomere length was 1, notably shorter than the adjacent normal thyroid tissue. **C:** Dot plots of semiquantitative FISH assessments of telomere lengths in thyroid tumors. Comparisons of means using Student's *t*-tests showing a significant difference are indicated with their respective *P* values. $^{*}P < 0.02$, $^{**}P < 0.006$, $^{***}P < 0.005$, $^{****}P < 0.002$, and $^{*****}P < 0.0001$. Means and standard deviations are shown.

Table 2. Telomere Length in Thyroid Tumors

Telomere length	Malignant tumors			Benign tumors	
	PTC (n = 15)	FC/HC (n = 7)	FVPTC (n = 12)	FA/HA (n = 18)	AN (n = 9)
0 (very short)	4 (27%)	1 (14%)	1 (8%)	0	0
1 (notably shorter than normal)	8 (53%)	3 (43%)	3 (25%)	7 (39%)	2 (22%)
2 (similar to normal)	3 (20%)	3 (43%)	8 (67%)	11 (61%)	0
3 (notably longer than normal)	0	0	0	0	7 (88%)
4 (very long)	0	0	0	0	0

%FL-*hTERT* and telomere length in thyroid tumors (Figure 4C), with the bivariate linear fit showing a Spearman correlation coefficient of −0.4 ($P < 0.004$).

Classifying Thyroid Tumors Using Telomere Length and %FL-hTERT

We further investigated whether the telomerase transcript variant expression patterns and telomere-length results could be used to classify thyroid tumors. We used the standard pathologic classification of thyroid tumors into benign (FA, HA, and AN) and malignant (PTC, FC, HC, and FVPTC) subtypes, and we determined how combinations of telomere length and %FL-*hTERT* would stratify the cases.

For this analysis, *hTERT* expression and telomere length were examined separately and in combination for their ability to distinguish between histopathologically defined malignant (n = 34) and benign (n = 27) thyroid tumor subtypes. Overall, on average, the malignant tumors showed a higher percentage of full-length *hTERT* expression (mean ± SE: 50.26 ± 7.37) and short telomere lengths (mean ± SE: 1.24 ± 0.13) compared with benign tumors, which showed a lower %FL-*hTERT* (mean ± SE: 18.47 ± 4.95) and longer telomere lengths (mean ± SE: 1.93 ± 0.15). When examining expression alone, a higher full-length *hTERT* fraction was associated with a significantly higher odds of malignancy per unit increase in expression compared with benign tumor subtypes (odds ratio = 1.03, 95% confidence interval = 1.01–1.04; P = 0.004).

Figure 5 summarizes the ROC curves obtained for %FL-*hTERT* expression, telomere length, and their combined use in distinguishing histopathologically defined malignant from benign thyroid tumors. Using a %FL-*hTERT* of 33% or greater to define malignancy, the ROC curve showed an AUC of 0.70, corresponding to a sen-

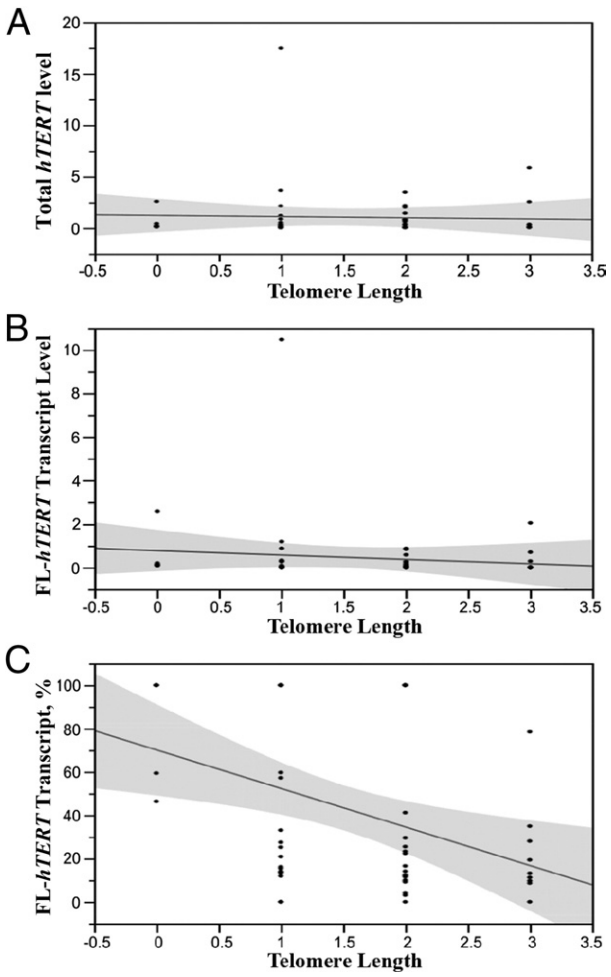

Figure 4. Correlation between *bTERT* variant expression and telomere length in thyroid tumors. Scatterplots showing the bivariate linear fit and 95% confidence intervals between *bTERT* levels and telomere length assessed by FISH analysis are shown. **A:** Total *bTERT* expression assessed by quantitative RT-PCR. Spearman's correlation coefficient was −0.1 ($P > 0.5$). **B:** *bTERT* full-length transcript levels assessed by quantitative RT-PCR. Spearman's correlation coefficient was −0.3 ($P > 0.06$). **C:** Percentage of full-length transcription expression. Spearman's correlation coefficient was −0.4 ($P < 0.0041$).

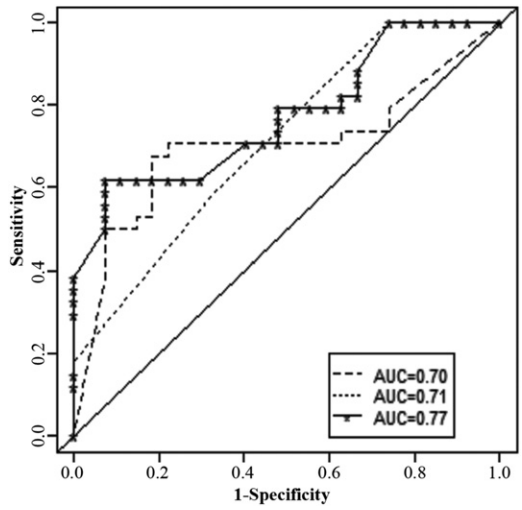

Figure 5. ROC analysis of %FL-*bTERT* and telomere length. ROC curves for distinguishing malignant versus benign thyroid tumor types using %FL-*bTERT* expression (**dashed line**), telomere length (**dotted line**), and combined %FL-*bTERT* expression and telomere length (**solid line**). The **diagonal line** denotes an AUC = 0.50.

sitivity of 0.53 and a specificity of 0.85. In terms of telomere length, a longer length was associated with significantly lower odds of malignancy per unit increase in length compared with benign thyroid tumor subtypes (odds ratio = 0.29, 95% confidence interval = 0.13 to 0.66; $P = 0.003$). The ROC curve showed an AUC of 0.71, corresponding to a sensitivity of 0.59 and a specificity of 0.67, based on a telomere length of <2 to define malignancy.

To examine the combined use of information from %FL-*hTERT* expression and telomere length, a multivariable model was developed. For this model, %FL-*hTERT* was associated with significantly increased odds of malignant compared with benign tumor types (odds ratio = 1.02, 95% confidence interval = 1.00 to 1.04; $P = 0.03$) per unit increase while adjusting for telomere length. A longer telomere length was associated with a significantly decreased odds of malignancy compared with benign tumors per unit increase, adjusting for %FL-*hTERT* (odds ratio = 0.36, 95% confidence interval = 0.15 to 0.84; $P = 0.02$). With the combined use of information from %FL-*hTERT* and telomere length, we obtained an AUC of 0.77, which did not constitute a significant improvement over the separate use of information from %FL-*hTERT* ($P = 0.19$) or telomere length ($P = 0.11$; Figure 5).

Discussion

Numerous studies in the past two decades have revealed that telomere alteration and telomerase activation are among the most important mechanisms in carcinogenesis and tumor progression. Some investigators provide evidence that telomerase is involved in tumorigenesis mainly through the maintenance of telomeres in tumor cells.[24,39–41] Recent studies also demonstrated alternative telomere maintenance mechanisms in human cells, although these seem to be operative much less frequently, particularly in epithelial carcinomas.[41–46] In this study, we investigated *hTERT* expression in benign and malignant thyroid tumors using three measures. We first measured total *hTERT* transcript levels using a PCR probe that did not discriminate between alternative splice variants. We also focused on the active full-length isoform in absolute terms and in relation to inactive or inhibitory splice variants present. Finally, we studied the telomere length and its correlation with *hTERT* expression and splice variant patterns. We chose a nested PCR approach to increase the sensitivity to detect the patterns of *hTERT* alternative splice transcripts. The PCR conditions were optimized using thyroid cell lines to minimize any distortion in the amplified product ratio. To maintain a linear quantitative relationship between the amount of final amplified product and the amount of target sequence in the nested PCR, the first-round PCR was limited to the exponential phase of the reaction.[29,47,48]

The approach used to quantify telomere length on permanent paraffin-embedded tissue sections was validated in our laboratories[19,20] and is based on a PNA-based FISH assay. The probe we use in telomere-specific FISH is a relatively small, directly labeled PNA probe with superior hybridization properties, eg, the ability to hybridize in very low salt conditions, that prevent competitive re-annealing of the target genomic DNA sequences compared with more traditional FISH techniques that use DNA or RNA hybridization probes. Our use of a directly labeled PNA probe targeting a genomic tandem repeat sequence also allows us to avoid the use of secondary reagents (antibodies, etc) for signal detection and/or signal amplification that could potentially create difficulties with detection reagent access and potential loss of signal linearity. The FISH analysis was performed in a blinded manner, and the tumor subtype was not readily discernible under fluorescence while the telomere length was assessed. We also performed careful intraobserver and interobserver validation to make sure that we could report valid results. The detectable length of telomeres, particularly in a clinical sample, depends on a variety of factors, including the history of the tissue regarding when previous cell generations had to break through the Hayflick limit imposed by ever-shortening telomeres, and the state of regulation of telomerase activity, which ultimately determines how much of the progressive telomere shortening incurred in previous generations of proliferation is reversed when telomerase is reactivated under the very high selection pressure encountered during carcinogenesis. The present data agree with previous studies that show that malignant epithelial tumors have relatively short telomeres and overexpress *hTERT* compared with benign and normal tissues.[49–52] These findings support the hypothesis that *hTERT* reexpression is induced by the feedback signal of telomere shortening. Many studies have focused on telomerase enzyme activity, which is highly dependent on assay conditions and sample preservation. Furthermore, most *hTERT* expression studies published to date have measured overall *hTERT* transcripts and do not distinguish among the different *hTERT* splice isoforms. The present data indicate that overall *hTERT* and active full-length isoform expression can reliably distinguish only PTCs from other thyroid tumor subtypes (Figure 1, A and B), although the low number of FCs in this study precludes any robust conclusions for that subset. However, the fraction of active full-length transcript, expressed as percentage of total *hTERT* expression (%FL-*hTERT*, Figure 2C) classified the thyroid tumors into three groups: i) PTC, HC, and FC; ii) FVPTC, HA, and FA; and iii) AN. This classification was also found by assessing relative telomere length. The morphologic similarities of FCs, FVPTCs, and FAs support the notion that some of these follicular lesions are neither clearly benign nor malignant but may represent a continuum, and reliable subclassification may be achieved only if diagnostic molecular and genetic markers can be developed.[53,54] Indeed, these follicular lesions are notoriously difficult to classify pathologically in a reliable manner, with interobserver variability reported up to 60%.[55–57] In one study, eight pathologists were asked to review the same slides from 21 follicular lesions, and complete agreement was achieved in only 2 cases,[58] indicating that these lesions as a whole remain diagnostically challenging. Furthermore, follicular lesions have been shown to bear some genetic similarity,

and overlap between benign and malignant thyroid tumors has been found in many studies including single nucleotide polymorphism analysis, molecular marker detection, and microarray profiling.[53,54,59] The presence of specific molecular markers, including *PAX8-PPARγ, RET/PTC, RAS*, and *CK19* in some histologically benign nodules may suggest that some of these tumors harbor malignant potential.[60–63] Available evidence also suggests that even some histologically very benign-appearing thyroid lesions could actually have malignant potential.[64] In the present study, the %FL-*hTERT* isoform was very low in eight of nine ANs. One AN showed 34.93% of the full-length isoform. On FNA cytology, this tumor was suspicious for PTC, with focal atypia, nuclear grooves, and elongation and may, thus, have represented an occult microcarcinoma missed on permanent section by sampling error. Furthermore, this patient had a history of breast and cervical cancer and a family history remarkable for multiple malignancies in her father (breast and liver) and one of her two sisters (lung and pancreas) and multiple additional cancers in her extended family. Although speculative, it is possible that this patient's *hTERT* phenotype may have had a genetic component. Because ANs and FAs are also part of a morphologic continuum rather than distinct entities, biomarkers such as %FL-*hTERT* may have value in further categorizing these lesions and their malignant potential.

The reported contradictory findings of telomere length, telomerase activity, and *hTERT* expression in benign and malignant tumors have added to the complexity of telomere biology in human tumorigenesis, including thyroid cancer.[24,65,66] One explanation for some of these discrepancies could be related to the regulation of telomerase activity by *hTERT* alternative splicing, or more specifically, the fraction of expressed telomerase peptides that consists of inhibitory or inactive peptides. The α-deletion transcript leads to dominantly negative regulation of telomerase activity.[32,33] The β- and α-β-deletion variants may produce truncated nonfunctional proteins or trigger nonsense-mediated mRNA decay because of the premature stop codons.[33,35,67] In agreement with the previous studies, we found no correlation between telomere length and overall *hTERT* expression and only a weak correlation even with absolute full-length expression levels. The present data demonstrate, however, that telomere length was clearly associated with the percentage of *hTERT* full-length isoform, the isoform that may correlate best with telomerase activity, as reported previously.[29] We did not have sufficient tissue to repeat the assessment of telomerase enzymatic activity because this work was focused on the diagnostically challenging small early-stage tumors. The present results contrast with a recent study finding no significant correlation between telomere length and telomerase activity in established melanoma cell lines.[67] This may be a reflection of the profound changes cells undergo during their adaptation to tissue culture growth. These results are in line with the notion that telomerase activity is required to overcome the chromosome instability caused by short telomeres. Absolute levels of full-length *hTERT* may be confounded either by additional translational modulation or by concomitant production of inhibitory peptides from alternative splice variants and may, therefore, not be precisely correlated with telomerase activity. This would also be consistent with earlier results suggesting that telomerase activity would be a useful biomarker to distinguish benign from malignant follicular neoplasms,[68] indicating that enzymatic assays of telomerase activity, although technically more challenging, more closely reflect telomerase function and the state of telomere function in cancer cells than measures of overall *hTERT* transcript levels that have shown considerable overlap between benign and malignant tumors in many organs.

The present data confirm that most thyroid carcinomas have relatively short telomeres and overexpress *hTERT* compared with benign and normal tissues. We further demonstrate that telomere length is negatively correlated with the percentage of full-length *hTERT* transcript but not with absolute expression levels of full-length *hTERT* transcript or overall *hTERT* expression levels. Moreover, high fractions of full-length *hTERT* transcripts are associated with FCs and PTCs. This is consistent with the concept that tumors that have reached a stage of critically short telomeres require enzymatically active telomerase for continued proliferation, as reflected by a high fraction of full-length *hTERT* transcript.

To our knowledge, this is the first study on the association of telomere length and *hTERT* alternative splice variant patterns in thyroid tumors. The correlation of telomere length with the expression patterns of *hTERT* alternative splice variants described herein provides further insights into telomere biology in thyroid tumorigenesis.

Acknowledgments

We thank Dante Trusty and Kristen Talbot for expert technical support.

References

1. Altekruse SF, Kosary CL, Krapcho M, Neyman N, Aminou R, Waldron W, Ruhl J, Howlader N, Tatalovich Z, Cho H, Mariotto A, Eisner MP, Lewis DR, Cronin K, Chen HS, Feuer EJ, Stinchcomb DG, Edwards BK: SEER Cancer Statistics Review, 1975–2007. Bethesda, MD, National Cancer Institute, 2010
2. Chen AY, Jemal A, Ward EM: Increasing incidence of differentiated thyroid cancer in the United States, 1988–2005. Cancer 2009, 15: 3801–3807
3. Gharib H, Papini E: Thyroid nodules: clinical importance, assessment, and treatment. Endocrinol Metab Clin North Am 2007, 36:707–735, vi
4. Hay ID, Grant CS, Bergstralh EJ, Thompson GB, van Heerden JA, Goellner JR: Unilateral total lobectomy: is it sufficient surgical treatment for patients with AMES low-risk papillary thyroid carcinoma? Surgery 1998, 124:958–966
5. Mazzaferri EL, Jhiang SM: Long-term impact of initial surgical and medical therapy on papillary and follicular thyroid cancer. Am J Med 1994, 97:418–428
6. Clark OH, Levin K, Zeng Q, Greenspan FS, Siperstein A: Thyroid cancer: the case for total thyroidectomy. Eur J Can Clin Oncol 1988, 24:305–313
7. Baloch ZW, LiVolsi VA, Asa SL, Rosai J, Merino MJ, Randolph G, Vielh P, DeMay RM, Sidawy MK, Frable WJ: Diagnostic terminology and morphologic criteria for cytologic diagnosis of thyroid lesions: a synopsis of the National Cancer Institute Thyroid Fine-Needle Aspiration State of the Science Conference. Diagn Cytopathol 2008, 36:425–437

8. Gharib H, Goellner JR, Zinsmeister AR, Grant CS, Van Heerden JA: Fine-needle aspiration biopsy of the thyroid: the problem of suspicious cytologic findings. Ann Intern Med 1984, 101:25–28
9. Burch HB: Evaluation and management of the solid thyroid nodule. Endocrinol Metab Clin North Am 1995, 24:663–710
10. Goellner JR, Gharib H, Grant CS, Johnson DA: Fine needle aspiration cytology of the thyroid, 1980 to 1986. Acta Cytol 1987, 31:587–590
11. Chen H, Zeiger MA, Clark DP, Westra WH, Udelsman R: Papillary thyroid cancer: can operative management be solely based on fine needle aspiration? J Am Coll Surg 1997, 184:605–610
12. Yang GC, Liebeskind D, Messina AV: Should cytopathologists stop reporting follicular neoplasms on fine-needle aspiration of the thyroid? Cancer 2003, 99:69–74
13. Eszlinger M, Krohn K, Hauptmann S, Dralle H, Giordano TJ, Paschke R: Perspectives for improved and more accurate classification of thyroid epithelial tumors. J Clin Endocrinol Metab 2008, 93:3286–3294
14. Hemann MT, Strong MA, Hao LY, Greider CW: The shortest telomere, not average telomere length, is critical for cell viability and chromosome stability. Cell 2001, 107:67–77
15. Counter CM, Avilion AA, LeFeuvre CE, Stewart NG, Greider CW, Harley CB, Bacchetti S: Telomere shortening associated with chromosome instability is arrested in immortal cells which express telomerase activity. EMBO J 1992, 11:1921–1929
16. Bacchetti S: Telomere maintenance in tumour cells. Cancer Surv 1996, 28:197–216
17. Kawai T, Hiroi S, Nakanishi K, Meeker AK: Telomere length and telomerase expression in atypical adenomatous hyperplasia and small bronchioloalveolar carcinoma of the lung. Am J Clin Pathol 2007, 127:254–262
18. Rosenberg R, Gertler R, Stricker D, Lassmann S, Werner M, Nekarda H, Siewert JR: Telomere length and hTERT expression in patients with colorectal carcinoma. Recent Results Cancer Res 2003, 162:177–181
19. Meeker AK, Hicks JL, Platz EA, March GE, Bennett CJ, Delannoy MJ, De Marzo AM: Telomere shortening is an early somatic DNA alteration in human prostate tumorigenesis. Cancer Res 2002, 62:6405–6409
20. Meeker AK, Hicks JL, Gabrielson E, Strauss WM, De Marzo AM, Argani P: Telomere shortening occurs in subsets of normal breast epithelium as well as in situ and invasive carcinoma. Am J Pathol 2004, 164:925–935
21. van Heek NT, Meeker AK, Kern SE, Yeo CJ, Lillemoe KD, Cameron JL, Offerhaus GJ, Hicks JL, Wilentz RE, Goggins MG, De Marzo AM, Hruban RH, Maitra A: Telomere shortening is nearly universal in pancreatic intraepithelial neoplasia. Am J Pathol 2002, 161:1541–1547
22. Stewart SA: Telomere maintenance and tumorigenesis: an "ALT"ernative road. Curr Mol Med 2005, 5:253–257
23. Henson JD, Hannay JA, McCarthy SW, Royds JA, Yeager TR, Robinson RA, Wharton SB, Jellinek DA, Arbuckle SM, Yoo J, Robinson BG, Learoyd DL, Stalley PD, Bonar SF, Yu D, Pollock RE, Reddel RR: A robust assay for alternative lengthening of telomeres in tumors shows the significance of alternative lengthening of telomeres in sarcomas and astrocytomas. Clin Cancer Res 2005, 11:217–225
24. Kammori M, Takubo K, Nakamura K, Furugouri E, Endo H, Kanauchi H, Mimura Y, Kaminishi M: Telomerase activity and telomere length in benign and malignant human thyroid tissues. Cancer Lett 2000, 159:175–181
25. Czerlinski G, Ypma T: Mechanisms of telomerase-dimer catalysis. J Theor Biol 2008, 250:512–523
26. Wenz C, Enenkel B, Amacker M, Kelleher C, Damm K, Lingner J: Human telomerase contains two cooperating telomerase RNA molecules. EMBO J 2001, 20:3526–3534
27. Kilian A, Bowtell DD, Abud HE, Hime GR, Venter DJ, Keese PK, Duncan EL, Reddel RR, Jefferson RA: Isolation of a candidate human telomerase catalytic subunit gene, which reveals complex splicing patterns in different cell types. Hum Mol Genet 1997, 6:2011–2019
28. Hisatomi H, Ohyashiki K, Ohyashiki JH, Nagao K, Kanamaru T, Hirata H, Hibi N, Tsukada Y: Expression profile of a γ-deletion variant of the human telomerase reverse transcriptase gene. Neoplasia 2003, 5:193–197
29. Wang Y, Kowalski J, Tsai HL, Marik R, Prasad N, Somervell H, Lo PK, Sangenario LE, Dyrskjot L, Orntoft TF, Westra WH, Meeker AK, Eshleman JR, Umbricht CB, Zeiger MA: Differentiating alternative splice variant patterns of human telomerase reverse transcriptase in thyroid neoplasms. Thyroid 2008, 18:1055–1063
30. Fan Y, Liu Z, Fang X, Ge Z, Ge N, Jia Y, Sun P, Lou F, Bjorkholm M, Gruber A, Ekman P, Xu D: Differential expression of full-length telomerase reverse transcriptase mRNA and telomerase activity between normal and malignant renal tissues. Clin Cancer Res 2005, 11:4331–4337
31. Ulaner GA, Hu J-F, Vu TH, Ciudice LC, Hoffman AR: Telomerase activity in human development is regulated by human telomerase reverse transcriptase (hTERT) transcription and by alternate splicing of hTERT transcripts. Cancer Res 1998, 58:4168–41672
32. Colgin LM, Wilkinson C, Englezou A, Kilian A, Robinson MO, Reddel RR: The hTERTalpha splice variant is a dominant negative inhibitor of telomerase activity. Neoplasia 2000, 2:426–432
33. Yi X, White DM, Aisner DL, Baur JA, Wright WE, Shay JW: An alternate splicing variant of the human telomerase catalytic subunit inhibits telomerase activity. Neoplasia 2000, 2:433–440
34. Nguyen BN, Elmore LW, Holt SE: Mechanism of dominant-negative telomerase function. Cell Cycle 2009, 8:3227–3233
35. Wick M, Zubov D, Hagen G: Genomic organization and promoter characterization of the gene encoding the human telomerase reverse transcriptase (hTERT). Gene 1999, 232:97–106
36. Brambilla C, Folini M, Gandellini P, Daprai L, Daidone MG, Zaffaroni N: Oligomer-mediated modulation of hTERT alternative splicing induces telomerase inhibition and cell growth decline in human prostate cancer cells. Cell Mol Life Sci 2004, 61:1764–1774
37. Chen C, Hong YK, Ontiveros SD, Egholm M, Strauss WM: Single base discrimination of CENP-B repeats on mouse and human Chromosomes with PNA-FISH. Mamm Genome 1999, 10:13–18
38. DeLong ER, DeLong DM, Clarke-Pearson DL: Comparing the areas under two or more correlated receiver operating characteristic curves: a nonparametric approach. Biometrics 1988, 44:837–845
39. Bacchetti S, Counter CM: Telomere and telomerase in human cancer. Int J Oncol 1995, 7:423–432
40. Greider CW: Telomere length regulation. Annu Rev Biochem 1996, 65:337–365
41. Opitz OG: Telomeres, telomerase and malignant transformation. Curr Mol Med 2005, 5:219–226
42. Subhawong AP, Heaphy CM, Argani P, Konishi Y, Kouprina N, Nassar H, Vang R, Meeker AK: The alternative lengthening of telomeres phenotype in breast carcinoma is associated with HER-2 overexpression. Mod Pathol 2009, 22:1423–1431
43. Stadler G, Wieser M, Streubel B, Stift A, Friedl J, Gnant M, Niederle B, Beham A, Katinger H, Pfragner R, Grillari J, Voglauer R: Low telomerase activity: possible role in the progression of human medullary thyroid carcinoma. Eur J Cancer 2008, 44:866–875
44. Fasching CL, Bower K, Reddel RR: Telomerase-independent telomere length maintenance in the absence of alternative lengthening of telomeres-associated promyelocytic leukemia bodies. Cancer Res 2005, 65:2722–2729
45. Gertler R, Rosenberg R, Stricker D, Friederichs J, Hoos A, Werner M, Ulm K, Holzmann B, Nekarda H, Siewert JR: Telomere length and human telomerase reverse transcriptase expression as markers for progression and prognosis of colorectal carcinoma. J Clin Oncol 2004, 22:1807–1814
46. Neumann AA, Reddel RR: Telomere maintenance and cancer: look, no telomerase. Nat Rev Cancer 2002, 2:879–884
47. Haff LA: Improved quantitative PCR using nested primers. PCR Methods Appl 1994, 3:332–337
48. Takahashi T, Tamura M, Takahashi SN, Matsumoto K, Sawada S, Yokoyama E, Nakayama T, Mizutani T, Takasu T, Nagase H: Quantitative nested real-time PCR assay for assessing the clinical course of tuberculous meningitis. J Neurol Sci 2007, 255:69–76
49. Saji M, Westra WH, Chen H, Umbricht CB, Tuttle RM, Box MF, Udelsman R, Sukumar S, Zeiger MA: Telomerase activity in the differential diagnosis of papillary carcinoma of the thyroid. Surgery 1997, 122:1137–1140
50. Umbricht CB, Conrad GT, Clark DP, Westra WH, Smith DC, Zahurak M, Saji M, Smallridge RC, Goodman S, Zeiger MA: Human telomerase reverse transcriptase gene expression and the surgical management of suspicious thyroid tumors. Clin Cancer Res 2004, 10:5762–5768
51. Mora J, Lerma E: Telomerase activity in thyroid fine needle aspirates. Acta Cytol 2004, 48:818–824

52. Liou MJ, Chan EC, Lin JD, Liu FH, Chao TC: Human telomerase reverse transcriptase (hTERT) gene expression in FNA samples from thyroid neoplasms. Cancer Lett 2003, 191:223–227
53. Arora N, Scognamiglio T, Lubitz CC, Moo TA, Kato MA, Zhu B, Zarnegar R, Chen YT, Fahey TJ III: Identification of borderline thyroid tumors by gene expression array analysis. Cancer 2009, 115:5421–5431
54. Barden CB, Shister KW, Zhu B, Guiter G, Greenblatt DY, Zeiger MA, Fahey TJ III: Classification of follicular thyroid tumors by molecular signature: results of gene profiling. Clin Cancer Res 2003, 9:1792–1800
55. Zeiger MA, Dackiw AP: Follicular thyroid lesions, elements that affect both diagnosis and prognosis. J Surg Oncol 2005, 89:108–113
56. Renshaw AA, Gould EW: Why there is the tendency to "overdiagnose" the follicular variant of papillary thyroid carcinoma. Am J Clin Pathol 2002, 117:19–21
57. Lloyd RV, Erickson LA, Casey MB, Lam KY, Lohse CM, Asa SL, Chan JK, DeLellis RA, Harach HR, Kakudo K, LiVolsi VA, Rosai J, Sebo TJ, Sobrinho-Simoes M, Wenig BM, Lae ME: Observer variation in the diagnosis of follicular variant of papillary thyroid carcinoma. Am J Surg Pathol 2004, 28:1336–1340
58. Hirokawa M, Carney JA, Goellner JR, DeLellis RA, Heffess CS, Katoh R, Tsujimoto M, Kakudo K: Observer variation of encapsulated follicular lesions of the thyroid gland. Am J Surg Pathol 2002, 26:1508–1514
59. Vasko VV, Gaudart J, Allasia C, Savchenko V, Di Cristofaro J, Saji M, Ringel MD, De Micco C: Thyroid follicular adenomas may display features of follicular carcinoma and follicular variant of papillary carcinoma. Eur J Endocrinol 2004, 151:779–786
60. Lacroix L, Lazar V, Michiels S, Ripoche H, Dessen P, Talbot M, Caillou B, Levillain JP, Schlumberger M, Bidart JM: Follicular thyroid tumors with the PAX8-PPARγ1 rearrangement display characteristic genetic alterations. Am J Pathol 2005, 167:223–231
61. Ishizaka Y, Kobayashi S, Ushijima T, Hirohashi S, Sugimura T, Nagao M: Detection of retTPC/PTC transcripts in thyroid adenomas and adenomatous goiter by an RT-PCR method. Oncogene 1991, 6:1667–1672
62. Vasko V, Ferrand M, Di Cristofaro J, Carayon P, Henry JF, de Micco C: Specific pattern of RAS oncogene mutations in follicular thyroid tumors. J Clin Endocrinol Metab 2003, 88:2745–2752
63. Cerilli LA, Mills SE, Rumpel CA, Dudley TH, Moskaluk CA: Interpretation of RET immunostaining in follicular lesions of the thyroid. Am J Clin Pathol 2002, 118:186–193
64. Arora N, Scognamiglio T, Zhu B, Fahey TJ III: Do benign thyroid nodules have malignant potential? an evidence-based review. World J Surg 2008, 32:1237–1246
65. Cristofari G, Lingner J: Telomere length homeostasis requires that telomerase levels are limiting. EMBO J 2006, 25:565–574
66. Matthews P, Jones CJ, Skinner J, Haughton M, de Micco C, Wynford-Thomas D: Telomerase activity and telomere length in thyroid neoplasia: biological and clinical implications. J Pathol 2001, 194:183–193
67. Lincz LF, Mudge LM, Scorgie FE, Sakoff JA, Hamilton CS, Seldon M: Quantification of hTERT splice variants in melanoma by SYBR green real-time polymerase chain reaction indicates a negative regulatory role for the β deletion variant. Neoplasia 2008, 10:1131–1137
68. Umbricht CB, Saji M, Westra WH, Udelsman R, Zeiger MA, Sukumar S: Telomerase activity: a marker to distinguish follicular thyroid adenoma from carcinoma. Cancer Res 1997, 57:2144–2147